ELSEVIER

Sensors and Actuators B 69 (2000) 144–152

SENSORS AND ACTUATORS B CHEMICAL

www.elsevier.nl/locate/sensorb

Effect of particle size and dopant on properties of SnO_2-based gas sensors

Gong Zhang, Meilin Liu *

School of Materials Science and Engineering, Georgia Institute of Technology, Atlanta, GA 30332-0245, USA

Received 10 December 1999; received in revised form 10 May 2000; accepted 16 May 2000

Abstract

The effect of composition, microstructure, and defect chemistry on sensing performance of gas sensors based on CuO-doped SnO_2 is investigated using sol–gel derived nano-sized powders (about 20 nm). The particle size of copper oxide doped tin oxide is varied by annealing at different temperatures and a significant grain growth is observed at temperatures above 1000°C due to the liquid phase sintering effect of copper oxide. The reduction of particle size to nanometers, or to the dimension comparable to the thickness of charge depletion layer, leads to a dramatic improvement in sensitivity and speed of response. It appears that the substitution of Sn by Cu in the cassiterite structure increases the concentration of oxygen vacancies and decreases the concentration of free electrons. In particular, the existence of cuprous ions (Cu^+), due to partial reduction of Cu^{2+} during sintering, plays an important role in enhancing the sensor response to nitric oxide (NO) and CO_2.

Keywords: SnO_2; CuO; Sol–gel; Nanostructure-material; Gas sensor

1. Introduction

Many pure and doped semiconducting oxides have been used for gas sensors, especially SnO_2-based materials due to its unique sensing properties. Modification of surface and bulk properties of tin oxide through doping of impurities is an effective way to improve sensitivity and selectivity [1,2]. Galdikas et al. [3] reported that the sensitivity of a tin oxide sensor was improved by small amounts of Cu sputtered on the surface. This effect is related to the induced surface states that were detected using XPS. Particle size and doping have also been reported [4] to influence the performance of SnO_2 gas sensors. Yamazeo and Miura [5] studied the effect of grain size on the sensitivity of SnO_2 gas sensors and concluded that the sensitivity to both CO and H_2 increased considerably as grain size was reduced. Li and Kawi [6] synthesized high surface area SnO_2 using a surfactant templating method and found that the sensitivity to H_2 increased linearly with the surface area of SnO_2. When particle size is reduced to nanometers, especially when the dimension of the crystallite is on the order of the thickness of the charge depletion layer, energy band bending is no longer restricted to the surface region, but extends into the bulk of the grains. In other words, the properties of the whole grain, not just the surface, may change completely due to solid–gas interaction. Accordingly, nanostructure is expected to have a dramatic influence on sensor performance. To date, however, copper oxide doped tin oxide with nanostructure for nitric oxide (NO) and CO_2 detection has not been reported yet. In this study, sol–gel derived CuO-doped SnO_2 nano-sized powders [7] are used to investigate the effect of nanostructure on its sensing characteristics to NO and CO_2 and possible sensing mechanisms are proposed.

2. Experimental

Nano-sized powders of pure SnO_2 were prepared as described elsewhere [7] and the powders of CuO-doped SnO_2 were prepared in a similar manner. Appropriate amounts (up to 50 mol%) of copper nitrate was added to the $SnCl_4$ sol solution as described for preparing pure

* Corresponding author. Tel.: +1-404-894-6114; fax: +1-404-894-9140.

E-mail address: meilin.liu@mse.gatech.edu (M. Liu).

0925-4005/00/$ - see front matter
PII: S0925-4005(00)00528-1

SnO_2 [7]. In order to investigate particle size dependence of sensor performance, the nano-sized powders were then annealed at different temperatures (800–1200°C) to vary the particle size. The annealed powders with desired particle sizes were then mixed with 5 wt.% of ethylene glycol (binder) and subsequently pressed into pellets (under a pressure of 2500 psi) to form porous sensing elements. Platinum pastes were screen-printed on both sides of the pellets and then fired at 650°C for 15 min to remove the binder. Structural and morphological changes of the powders were characterized using X-ray diffraction (XRD) (Philips PW-1800 X-ray diffractometer) and electron microscopy (Hitachi S-800 scanning electron microscope and Hitachi HF-2000 transmission electron microscope). Shown in Fig. 1 are the typical microstructures of the sensing elements (pellets pressed from powders) before sensor performance testing, which are essentially the same as that of the powders after annealing at different temperatures.

The sensing elements with platinum electrodes were placed in a tube furnace and a gas flow meter was used to control the flow rate of sample gases. The steady-state resistances (or conductances) of the sensing elements were determined using an EG&G potentiostat/galvanostat (273 A) interfaced with a computer. In a typical sensor response measurement, a constant voltage of 0.5 V was applied to each pellet while the corresponding steady-state

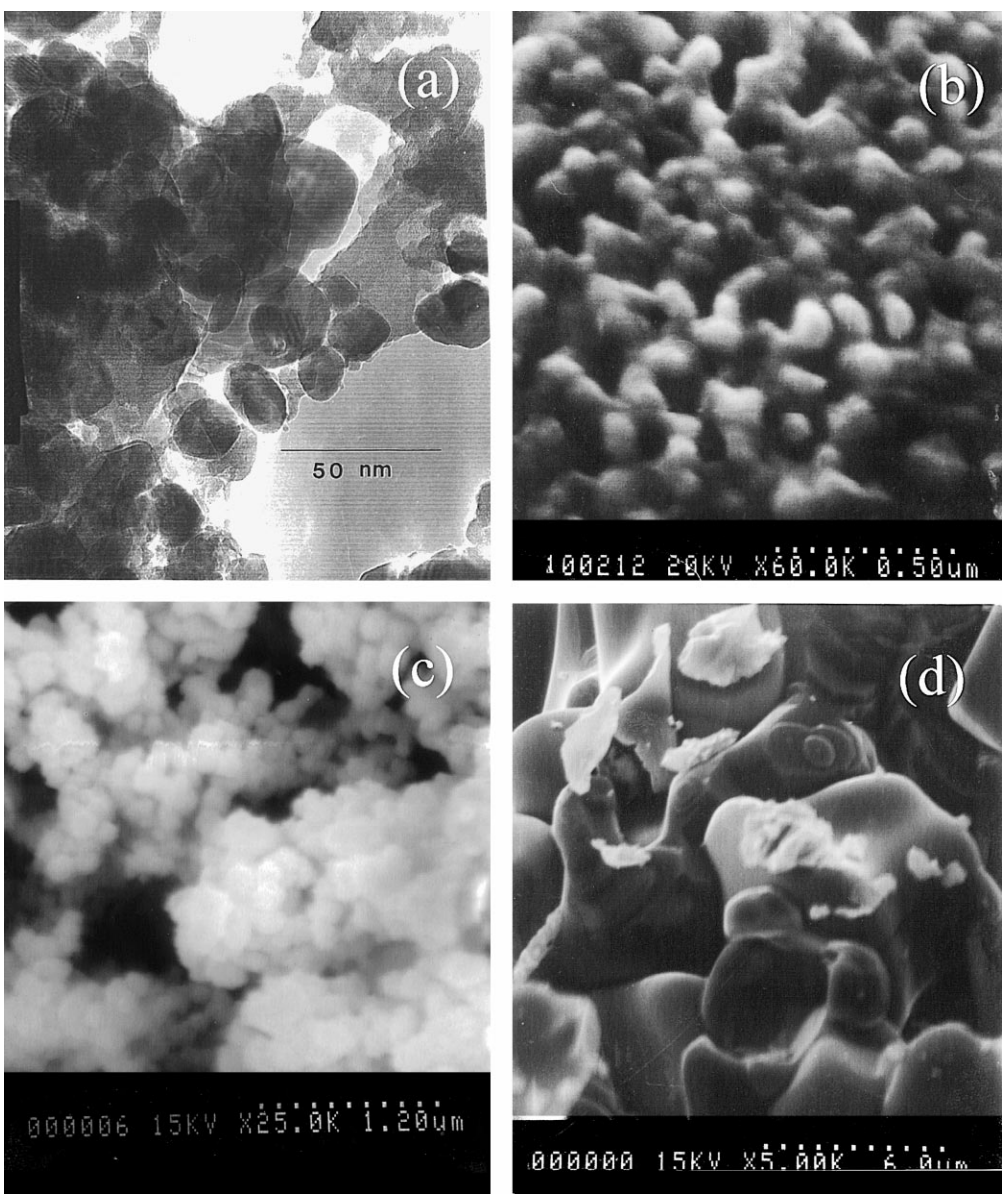

Fig. 1. TEM and SEM micrographs of SnO_2(CuO) as annealed at (a) 600°C (20 nm), (b) 800°C (100 nm), (c) 1000°C (290 nm), and (d) 1200°C (6 μm) in air for 2 h. The dimension in each parenthesis represents the average size of the SnO_2(CuO) particles.

current responses were recorded when different gases were flown through the test tube at a flow rate of 200 cm^3/min. Conductivities were calculated from the applied voltages, output currents, and the dimensions of the sensing elements (electrode area and pellet thickness).

3. Results

3.1. Morphology, microstructure, and composition

Fig. 1 shows the morphologies of SnO_2(CuO) powders annealed at different temperatures. The average particle size increased with annealing temperature from 20 nm at 600°C, to 100 nm at 800°C, to 290 nm at 1000°C, and to 6 μm at 1200°C. The surface area decreased accordingly with particle size or annealing temperature. The powders annealed at temperatures below 1000°C were highly porous which, in general, is preferred for gas sensor applications. To reveal the effect of copper oxide on sintering behavior of tin oxide, the particle sizes of pure SnO_2 samples and those of CuO-doped SnO_2 under the same firing conditions are shown in Fig. 2. It is evident that below 1000°C, there is little difference in particle size between them. Above 1000°C, however, a significant grain growth occurred in the SnO_2(CuO), due to a liquid-phase sintering effect of copper oxide. As studied by Dolet et al. [8], copper oxide was observed to melt between 1000°C and 1200°C, depending upon specific oxygen partial pressure. They observed the presence of copper-rich coagulated droplets on the surface of tin oxide sintered at 1150°C.

Shown in Fig. 3 are the XRD patterns of the SnO_2(CuO) powders fired for 2 h at 600°C, 800°C, and 1000°C, respectively, together with the standard XRD patterns for SnO_2, CuO, and Cu_2O. For the powders fired at 600°C, the observable peaks correspond to the cassiterite phase of SnO_2 and no peaks correspond to either CuO or Cu_2O phase, indicating that copper oxide is amorphous. For the powders annealed at temperature above 600°C, peaks of copper oxide become observable but intensities of the peaks remain low, suggesting that the concentration of copper oxide phase in the SnO_2(CuO) be small, far smaller than expected from that of its initial loading in the sol solution. There are two possible reasons in addition to the influence of the element scattering from tin: volatilization of copper oxide during sintering and doping of copper oxide into SnO_2. Labeau et al. [9] observed the volatilization of copper oxide during annealing at 800°C and attributed it to be the major source of copper oxide loss. Another possibility is that a considerable amount of copper ions dissolves into the tin oxide lattice. EDS analysis on a TEM of a single grain of CuO-doped SnO_2 shows that the average doping concentration of copper in tin oxide crystal annealed at 600°C is 15.6 mol%, which is much higher than that in SnO_2(CuO) solid solution previously reported, about 5% copper oxide [1,10]. This is most likely due to the different methods by which copper oxides were doped. Tin and copper ions were mixed at an atomic level in this study in the initial sol solution whereas the impregnation of copper ion solutions into tin oxide powder was generally adopted by other researchers [1,9]. In addition, the solubility of tin oxide in copper oxide was also studied by analyzing the composition of the copper enriched phase. Results indicated that the solubility of tin ions in copper oxide lattice was within the experimental error.

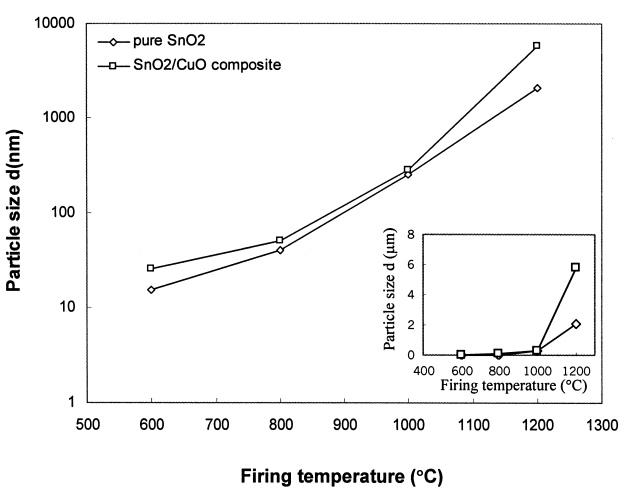

Fig. 2. Average particle sizes of pure SnO_2 and CuO-doped SnO_2 annealed at different temperatures in air for 2 h, showing the effect of copper oxide on the sintering behavior of SnO_2(CuO).

3.2. Sensor responses to NO, CO_2, and O_2

Shown in Fig. 4 are the responses of a SnO_2(CuO) sample, annealed at 600°C for 2 h, to different concentrations of NO in Ar measured at 200°C. The SnO_2(CuO) is more sensitive to NO than pure SnO_2. For example, when gas was switched from Ar to 1000 ppm NO in Ar, the resistance of SnO_2(CuO) changed by a factor of 4.3 whereas that of pure SnO_2 changed by a factor of 2.9. Even though SnO_2(CuO) and pure SnO_2 follow the same trend of change in the response time (i.e., the time required to reach 90% of the full response) with gas concentration, response time of SnO_2(CuO), 3 min, is much shorter than that of pure SnO_2, 18 min. In all cases, the output signals essentially recover to the original level, an indication of reversible interactions between the sensing elements and the gas to be detected. Fig. 5 shows the correlation between sensor responses and NO concentrations. Fig. 6 shows the effect of temperature on the responses of pure SnO_2 and SnO_2(CuO) with nanostructure (20 nm) in 1000 ppm NO. It is evident that the sensitivity of SnO_2(CuO) varies with operating temperature in a different way from that of pure SnO_2. While the sensitivity of SnO_2(CuO) to

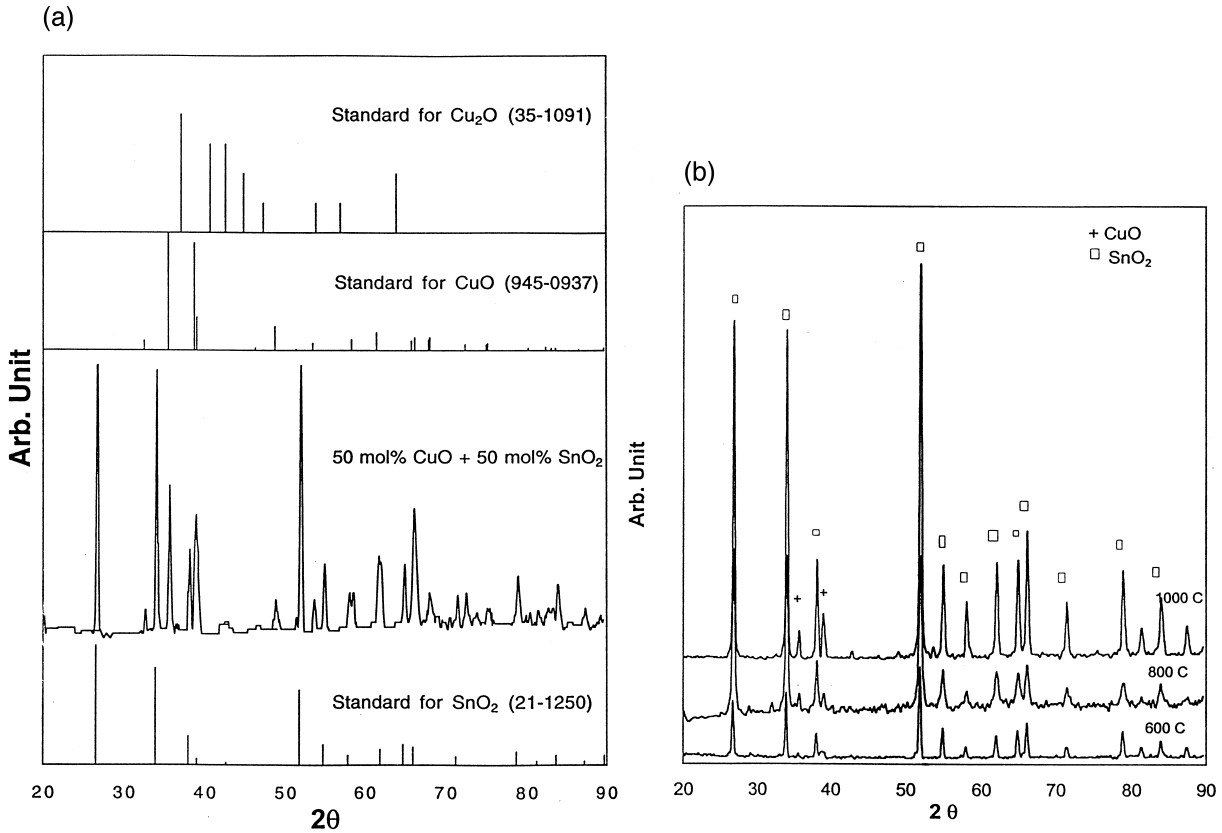

Fig. 3. XRD patterns of (a) standards for Cu_2O, CuO, and SnO_2, and physical mixture of CuO + SnO_2 and (b) SnO_2(CuO) annealed at different temperatures for 2 h.

NO reached a maximum at 200°C and then decreased with temperature thereafter, the pure SnO_2 exhibited an optimal sensitivity to NO at temperature around 300°C. This suggests that the underlying gas–solid interactions associated

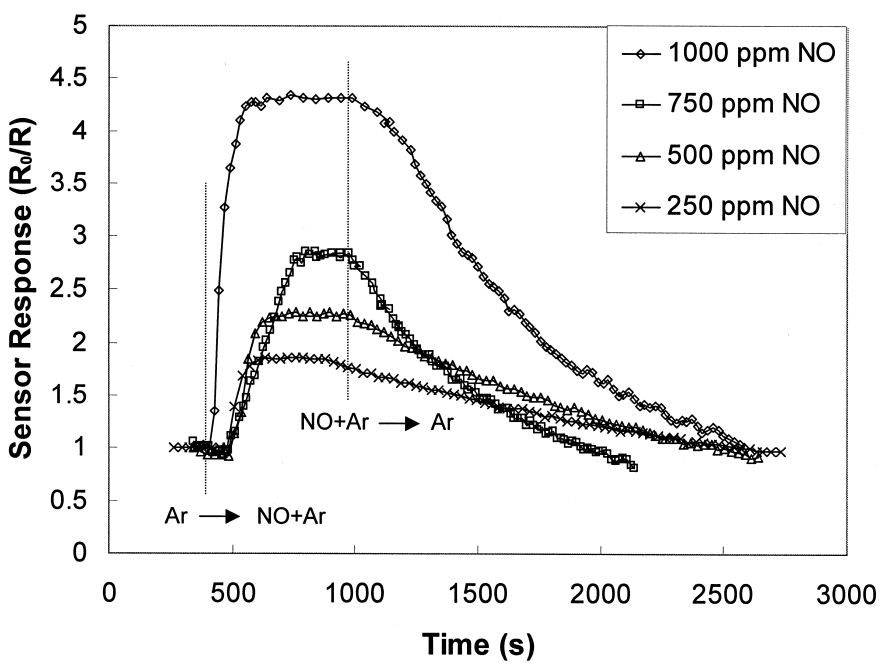

Fig. 4. Dynamic response to NO–Ar gas mixtures at 200°C of SnO_2(CuO) sensor with average grain size of 20 nm.

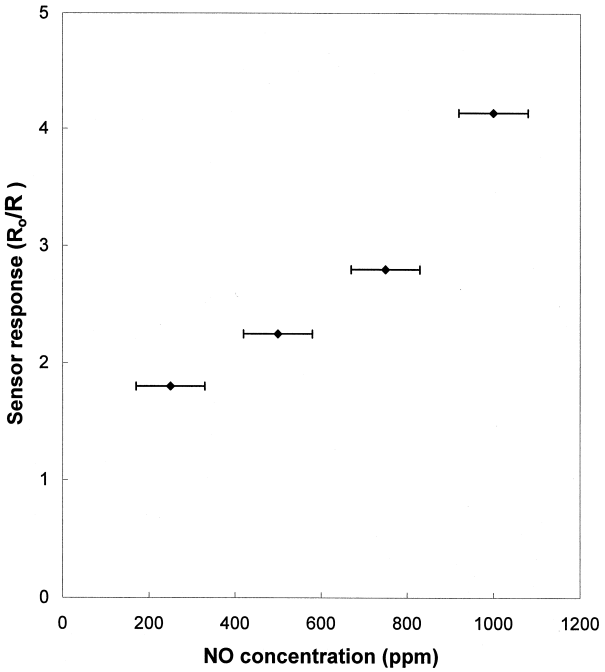

Fig. 5. Typical SnO_2(CuO) sensor responses to different concentrations of NO in Ar at 200°C. The average grain size of the SnO_2(CuO) sensor is 20 nm.

with different materials correspond to different characteristic temperatures. Accordingly, it is essential to carefully adjust the operating temperature of the sensor in order to obtain optimum performance to a specific gas species.

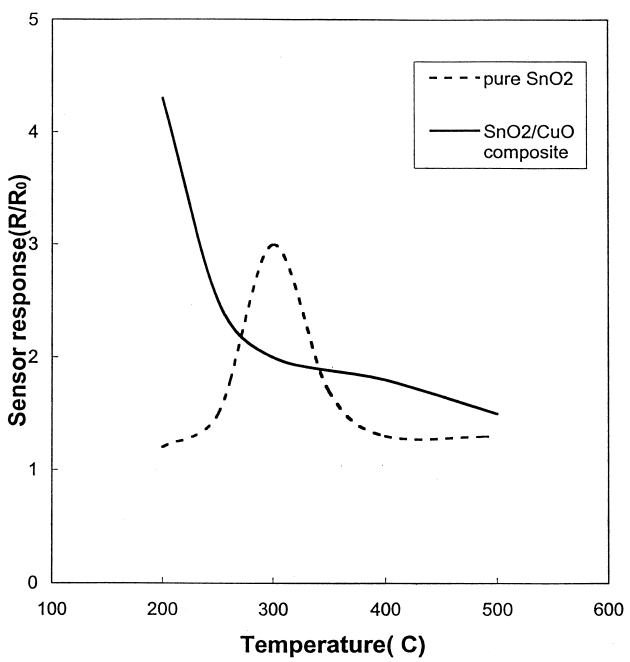

Fig. 6. Effect of temperature on the sensitivity of SnO_2(CuO) and pure SnO_2 annealed at 600°C for 2 h. The average particle size of the SnO_2(CuO) powder is 20 nm and the sensor responses were measured in 1000 ppm NO.

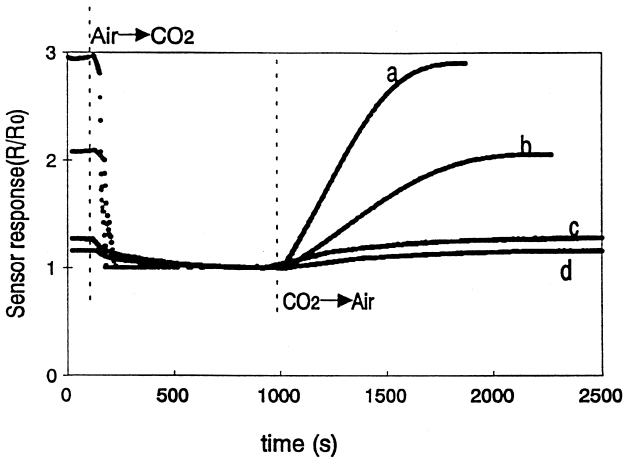

Fig. 7. Dynamic response of SnO_2(CuO) sensors annealed at different temperatures to CO_2 tested at 400°C. The microstructures of the sensors labeled as a, b, c, and d correspond to those shown in Fig. 1 labeled as a, b, c, and d.

Fig. 7 shows the dynamic response of the SnO_2(CuO) with different particle size to CO_2. The resistance of the sample increases fast within 1 min upon exposure to CO_2 switched from air. It is confirmed that the maximum sensor response decreases with particle size due to the decreased surface area. Fig. 8 shows that the sensor response of the material varied with CO_2 concentrations. Since oxygen plays an important role in the performance of tin oxide based gas sensor, the response of this sensing element to oxygen was also studied. Fig. 9 shows the dynamic response of SnO_2(CuO) with nanostructure (20 nm) to the change of

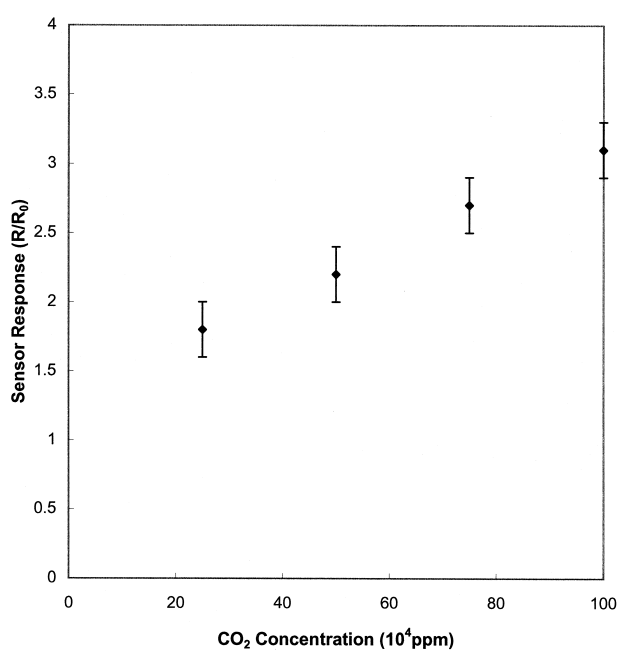

Fig. 8. Typical SnO_2(CuO) sensor response to different concentrations of CO_2 in Ar at 400°C. The average grain size of the SnO_2(CuO) sensor is 20 nm.

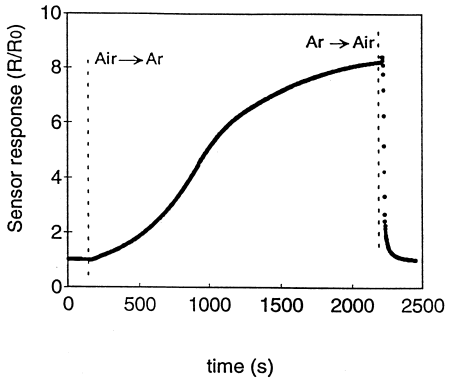

Fig. 9. Dynamic response of a SnO_2(CuO) sensor with grain size of 20 nm to oxygen at 400°C.

oxygen partial pressure (switched from argon to air). The resistance of the material decreased upon exposure to argon, indicating that SnO_2(CuO) is an n-type semiconducting oxide.

4. Discussion

4.1. Effect of particle size

The height of energy barrier to electron transport between neighboring grains in the SnO_2(CuO) is an important factor, which determines sensitivity of the material. The temperature dependence of conductivity of a semiconductor can be approximated by the Arrhenius equation [11],

$$\sigma = \sigma_0 \exp\left(\frac{-eV_s}{kT}\right), \tag{1}$$

where σ_0 is a factor that includes the bulk intragranular conductance, k the Boltzmann's constant, T the absolute temperature, and eV_s the potential energy barrier at the interface between two neighboring particles.

$$eV_s = \frac{e^2 N_t^2}{2\varepsilon_r \varepsilon_0 N_d}, \tag{2}$$

where N_t is the surface density of adsorbed oxygen ions (O_2^- or O^-), $\in_r \in_0$ the permittivity of the semiconductor, and N_d the volumetric density of the electron donors. Clearly, the energy barrier is a function of temperature, atmosphere (oxygen partial pressure), and dopant concentration; each of these parameters influences the energy barrier, the conductivity, and thus the sensitivity. Further, eV_s depends on particle size, especially when particle size is reduced to nanometers or in the order of the thickness of charge depletion layer (X_d). Different particle size corresponds to different ratio of X_d to the radius of the particles, provided that the absolute value of X_d is relatively independent of particle size. If the particle size is much larger than the X_d, the band bending resulting from the surface states X_d is restricted only to the surface region of the particle. If the particle size is reduced to nanometers (or on the order of X_d), however, the properties of the entire particles, not just the surfaces or interfaces, change dramatically due to solid–gas interactions, leading to a substantial improvement in sensor response. It is anticipated that both surface area and the ratio of charge depletion layer to the radius of particle will influence sensor responses. Thus, the sensitivity depends critically on particle size. The dependence of the energy barrier on particle size was studied as follows: the conductivities of the SnO_2(CuO) samples with different particle sizes were measured at temperatures from 150°C to 250°C in pure argon. It was found that the energy barrier, determined from the slope of the Arrhenius plots shown in Fig. 10, decreased with increasing particle size, implying that the sensitivity of the SnO_2(CuO) decreased with particle size.

4.2. Effect of doping

There are two possible positions, substitutional and interstitial, in the tin oxide lattice where copper ions can be introduced. In the first case, Cu^{2+} may substitute Sn^{4+} as follows,

$$CuO \overset{SnO_2}{\rightarrow} Cu''_{Sn} + O_0^x + V_0^{\cdot\cdot} \tag{3}$$

implying that substitution of Sn^{4+} by Cu^{2+} increases the oxygen vacancy concentration. At the same time, the equilibrium between solid and gas,

$$O_0^x \rightarrow \frac{1}{2}O_{2(g)} + 2e' + V_0^{\cdot\cdot} \tag{4}$$

requires that the free electron concentration decreases with the concentration of oxygen vacancies at a given oxygen partial pressure.

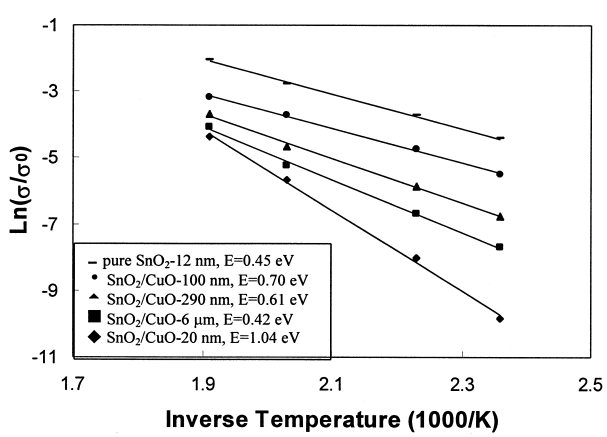

Fig. 10. Temperature dependence of conductivity of pure SnO_2 and SnO_2(CuO) with different particle sizes (annealed at different temperatures).

In the second case, the copper ions may occupy the interstitial sites in SnO_2 lattice according to the following defect reaction,

$$2CuO \xrightarrow{SnO_2} 2Cu_i^{\cdot\cdot} + 2O_0^x + V_{Sn}'''' \quad (5)$$

Further, the equilibrium for Schottky defects,

$$nil = V_{Sn}'''' + 2V_0^{\cdot\cdot} \quad (6)$$

implies that the increase in concentration of V_{Sn}'''' due to interstitial doping of copper ions results in a decrease in the concentration of oxygen vacancies and hence an increase of free electron concentration in tin oxide at a given oxygen partial pressure. The resistivity of pure SnO_2 measured at 600°C at a constant oxygen partial pressure (pure argon) was $2.4 \times 10^4\ \Omega$ cm and that of the CuO-doped tin oxide was $1.7 \times 10^4\ \Omega$ cm, implying that the copper ions substituted Sn at the regular lattice sites in tin oxide. It is more reasonable for copper ions to occupy substitutional than interstitial positions since the radii of Cu^{2+} and Sn^{4+} are 0.72 and 0.71 Å, respectively. The decrease in free electron concentration also resulted in an increase in X_d, thus increasing the energy barrier between adjacent grains.

4.3. Sensing mechanism

Sensor response depends mainly on the interactions between the sensing element and the gas to be detected. The interactions include physical and chemical adsorption. Physical adsorption refers to a surface adsorption caused by induced dipole–dipole or Van der Vaals interactions. Chemical adsorption, on the other hand, involves primary bonding or electrostatic interaction. The chemical interaction typically involves exchange electrons between adsorbed gas molecules and the metal oxide semiconductor, resulting in a change in band bending near interfaces and hence the electrical property of the sensing element.

The processes involved in a specific gas–metal oxide interaction may include formation of intermediate species, transport of species, and recombination with other species.

The first step is the formation of high-reactivity intermediate species such as dissociated atoms, free radicals, electrons, and excited molecules. Some transition metals or metal ions function as a catalyst to accelerate the speed of response of a sensor material to a specific gas. Another process is the movement of the intermediate species on the surface or into the bulk of the materials before recombination with either preadsorbed species on the surface or other defects in the bulk phase. These intermediate species will transport under the influence of a gradient in electrochemical potential if the activation site of the intermediate species is different from that of the recombination site. The recombination with other active species will complete the process of exchanging electrons between the sensing elements and the gas to be detected. The speed of sensor response is controlled by the slowest step, the rate-limiting step of the processes. Consequently, improving sensor performance depends on selecting a good catalyst to speed up the rate-limiting step and to minimize the average diffusion length of the intermediate species.

4.3.1. Oxidation state of Cu

The oxidation state of copper in SnO_2(CuO) is important since it influences the interaction with other gas species such as CO_2 [12] and NO [13]. Liu and Robota [14] observed that even under strongly oxidizing conditions, a significant fraction of the copper still remains as cuprous ions (Cu^+). In our study, copper and tin ions are homogeneously dispersed in the gel structure before firing. The local oxygen deficiency, when firing in steady air, may trigger the occurrence of the following reaction:

$$2CuO \rightarrow Cu_2O + \frac{1}{2}O_2 \uparrow \quad (7)$$

which reduces some Cu^{2+} to Cu^{1+} and thus, Cu^{2+} and Cu^+ coexist in the SnO_2(CuO). It is the Cu^+ ions in the material that play an important role in interaction with NO and CO_2.

4.3.2. NO detection

The catalytic reactions of NO over various transition metals have been extensively studied [13,15]. Especially for the catalyst containing copper ions, a redox mechanism associated with the valence change of copper was proposed [14]. Due to its high tendency of unpaired electrons to pair with another electron for bonding saturation, NO is adsorbed on active centers, Cu^+, and then reduced to NO^- radicals as Cu^+ is oxidized to Cu^{2+}. The highly active NO^- combines with the preadsorbed O^- on the surface of tin oxide to form NO_2 and at the same time the electrons are released to the conduction band of tin oxide. Only adsorbed O^- is taken into consideration in the interaction because of the low testing temperature, 200°C. At this temperature, it is difficult for NO^- to react directly with other species, such as O_0^x, O_2^-, and O^{2-} preadsorbed on the surface of SnO_2. In this process, the activation of NO gas molecules to active NO^- is an important step. This seems to be suggested by the comparative study of the dynamic responses of SnO_2(CuO) and pure SnO_2 to NO. The speed of response of pure SnO_2 to NO is much slower than that of SnO_2(CuO), due to the lack of the catalytic activation of NO over copper ions. Moreover, it seems that the copper in the tin oxide lattice helps to lower the desorption energy of the O^- preadsorbed on the tin oxide surface when gas was switched from Ar to 1000 ppm NO + Ar. The sensor response (R/R_0) was enhanced from 2.9 for pure SnO_2 to 4.3 for doped SnO_2 probably because more adsorbed O^- can be desorbed during the process. The temperature for maximum sensitivity to NO is 200°C for SnO_2(CuO) and 300°C for pure SnO_2. It seems that more energy is needed for the NO to grab O^-

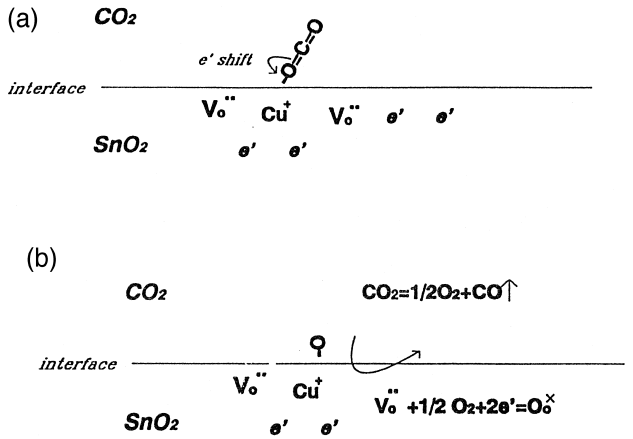

Fig. 11. Proposed mechanism of interaction between CO_2 gas molecules and SnO_2(CuO).

from the surface of tin oxide in the absence of copper oxide. Apparently, the copper ions play an important role in the interaction of NO with sensing materials and the desorption of O^-, greatly influencing the speed of response and sensitivity.

4.3.3. CO_2 detection

As schematically shown in Fig. 11, the detection mechanism is proposed as follows: some Cu^+ ions and oxygen vacancies are located on the surface of the sensing element. When CO_2 gas molecules are brought in contact with the sensing element, they are preferably adsorbed on the Cu^+ sites to form a bond between them due to the existence of an unshared electron pair in oxygen and an empty d orbital in Cu^+. As the electron cloud rearrangement is oriented toward Cu^+ side, which possesses higher electron affinity and eventually broken to release CO and O_2, the bond between oxygen and Cu^+ ions is weakened. The oxygen molecules then recombine with oxygen vacancies through the reaction $1/2O_2 + V_0^{\cdot\cdot} + 2'_e = O_0^x$, extracting two free electrons from the conduction band of tin oxide at the same time. This would decrease the conductivity of the sensing material.

When the gas was switched from air to argon, the maximum R/R_0 was about 8, which is merely due to the change in partial pressure of oxygen. When the gas exposed to the sensor was switched from pure air to pure carbon dioxide, the partial pressure of both oxygen and CO_2 was changed at the same time and the maximum R/R_0 was 4. Since the resistance of the sensing material increases with partial pressure of O_2 but decreases with the partial pressure of CO_2. the interaction between CO_2 and SnO_2(CuO) dominates the overall sensor response. Due to the ease of the bond formation between Cu^+ and CO_2 molecules, more CO_2 are absorbed, which pick up more electrons than are released from the desorption of oxygen. Thus, the net effect is dominated by the interaction between CO_2 and sensing material. Kinetically, the former reaction is more favorable than the latter one, as shown in Figs. 7 and 9. The response of the sensing materials to CO_2 is much faster than to O_2.

5. Conclusion

Doping of transition metal oxides to SnO_2 dramatically influences the defect chemistry and the sintering behavior of tin oxide. The substitution of Sn ions by copper ions created more oxygen vacancies in the material, leading to a decrease in the free electron concentration and an increase in sensitivity of the material. For example, when the sample gas is switched from Ar to 1000 ppm NO + Ar, the change in resistance of SnO_2(CuO) is 4.3 times while that of pure SnO_2 is 2.9 times. The response time of the former is about 3 min, whereas that of the later is 18 min. The improved sensor performance of doped SnO_2 over pure SnO_2 is due to the catalytic interaction of copper ion with the gas species to be detected. The temperature at which a sensor exhibits optimal sensitivity depends on the sensor material, 200°C for doped SnO_2 and 300°C for pure SnO_2. Further, it is found that, as the surface to volume ratio increases with decreasing particle size, both speed of response and sensitivity of a SnO_2(CuO) sensor are significantly improved.

Acknowledgements

The authors wish to gratefully acknowledge partial support of this project by NSF under Award No. DMR-9357520 and by the Georgia Tech Molecular Design Institute under prime contract N00014-95-1-1116 from the Office of Naval Research.

References

[1] A. Galdikas, A. Mironas, A. Setkus, Copper-doping level effect on sensitivity and selectivity of tin oxide thin film gas sensor, Sens. Actuators, B 26–27 (1995) 29–32.
[2] N. Butta, L. Cinquegrani, E. Mugno, A. Taglieuete, S. Pizzini, A family of tin oxide-based sensors with improved selectivity to methane, Sens. Actuators, B 6 (1992) 253–256.
[3] A. Galdikas, V. Jasutis, S. Kaciulis, G. Mattogno, A. Mironas, V. Olevano, D. Senuliene, A. Setkus, Peculiarities of surface doping with Cu in SnO_2 thin film gas sensors, Sens. Actuators, B 43 (1997) 140–146.
[4] C.N. Xu, J. Tamaki, N. Miura, N. Yamazoe, Grain size effects on gas sensitivity of porous SnO_2-based elements, Sens. Actuators, B 3 (1991) 147–155.
[5] N. Yamazeo, N. Miura, Some basic aspects of semiconductor gas sensor, in: S. Yamauchi (Ed.), Chemical Sensor Technology vol. 4 Kodansha, Tokyo, 1992, p. 19.
[6] G.J. Li, S. Kawi, High-surface-area SnO_2: a novel semiconductor-oxide gas sensor, Mater. Lett. 34 (1998) 99–102.
[7] G. Zhang, M. Liu, Preparation of nanostructured tin oxide using a sol–gel process based on tin tetrachloride and ethylene glycol, J. Mater. Sci. 34 (1999) 1–7.

[8] N. Dolet, J. Heintz, M. Onillon, J. Bonnet, Densification of 0.99 SnO_2 −0.01 CuO mixture: evidence for liquid phase sintering, J. Eur. Ceram. Soc. 9 (1992) 19–25.
[9] M. Labeau, U. Schmatz, G. Delabouglise, J. Roman, M. Vallet-Regi, A. Gaskov, Capacitance effects and gaseous adsorption on pure and doped polycrystalline tin oxide, Sens. Actuators, B 26–27 (1995) 49–52.
[10] J. Tamaki, T. Maekqwa, N. Miura, N. Yamazoe, CuO-SnO_2 element for highly sensitive and selective detection of H_2S, Sens. Actuators, B 9 (1992) 197–203.
[11] V. Lantto, P. Romppainen, S. Leppavuori, A study of the temperature dependence of the barrier energy in porous tin dioxide, Sens. Actuators 14 (1988) 149–163.
[12] R. Pirone, P. Ciambell, G. Moretti, G. Russo, Nitric oxide decomposition over Cu-exchange ZSM-5 with high Si/Al ratio, Appl. Catal., B 8 (1996) 197–207.
[13] M. Fernandez-Garcia, C.M. Alvarez, I. Rodriguez-Ramos, A. Guerrero-Ruiz, G.L. Haller, New insights on the mechanism of the NO reduction with CO over alumina-supported copper catalysts, J. Phys. Chem. 99 (1995) 16380–16382.
[14] D.J. Liu, H.J. Robota, In situ characterization of Cu-ZSM-% by X-ray absorption spectroscopy: SANES study of the copper oxidation state during selective catalytic reduction of nitric oxide by hydrocarbons, Appl. Catal., B 4 (1994) 155–165.
[15] N.Y. Topsoe, Mechanism of the selective catalytic reduction of nitric oxide by ammonia elucidated by in situ on-line Fourier transform infrared spectroscopy, Science 265 (26) (1994) 1217–1219, August.